Response of the magnetosphere-ionosphere system to a sudden southward turning of interplanetary magnetic field

Yiqun Yu[1] and Aaron J. Ridley[1]

Received 9 April 2008; revised 31 December 2008; accepted 12 January 2009; published 26 March 2009.

[1] A sudden southward turning of interplanetary magnetic field (IMF) is simulated by the University of Michigan's BATS-R-US model. The main goal of this study is to determine the time delay as well as physical processes between when an IMF discontinuity reaches the bow shock, when reconnection is initiated at the magnetopause, and when the ionosphere starts to react. While observations or empirical models might give an estimate of the time delay for the propagation of the discontinuity from the bow shock to the magnetopause, the global MHD simulation provides a more comprehensive insight of responses of the magnetosphere-ionosphere system. An idealized north-to-south IMF transition is modeled, using a solar wind velocity of 400 km/s. After the southward IMF encounters the bow shock, it takes about 6 min for the north-to-south IMF transition front to arrive at the subsolar geomagnetic field. The ionospheric response to this sudden southward IMF turning is delayed by another ~4 min, during which the magnetosphere undergoes a conversion from cusp reconnection to subsolar reconnection and the Alfvén wave propagation to the ionosphere takes place. Thereafter, changes in the ionosphere and ground magnetic perturbations associated with the southward IMF are observed. These responses appear to be globally onset as described in many other studies. The time it takes from the encounter of the IMF transition with the bow shock to when the ionospheric reaction takes place varies with the solar wind speed, ranging from nearly 15 min for a solar wind speed of 300 km/s to just over 6 min for solar wind speeds of 600 km/s.

Citation: Yu, Y., and A. J. Ridley (2009), Response of the magnetosphere-ionosphere system to a sudden southward turning of interplanetary magnetic field, *J. Geophys. Res.*, *114*, A03216, doi:10.1029/2008JA013292.

1. Introduction

[2] The response of the magnetosphere-ionosphere system to sudden southward turnings of the interplanetary magnetic field (IMF) have been studied by many researchers recently through observational data [*Ridley et al.*, 1998; *Ruohoniemi and Greenwald*, 1998; *Shepherd et al.*, 1999; *Murr and Hughes*, 2001; *Nishitani et al.*, 2002; *Lu et al.*, 2002] as well as simulations [*Lopez et al.*, 1999; *Slinker et al.*, 2001]. The main common idea from these studies is that the ionospheric electric potential responds globally to a sudden southward turning of IMF nearly simultaneously (<2 min), i.e., the initial changes in the dayside and nightside ionosphere show no significant difference in time, which is contrary to previous results that claimed that responses in the nightside are delayed from local noon owing to the propagation of the plasma convection from the dayside to the nightside [*Lockwood et al.*, 1986; *Todd et al.*, 1988; *Cowley and Lockwood*, 1992; *Saunders et al.*, 1992; *Khan and Cowley*, 1999]. Furthermore, *Murr and Hughes* [2001] and *Lu et al.* [2002] found that the reconfiguration of the system to the new condition depends on the local time.

[3] *Slinker et al.* [2001], *Ruohoniemi and Greenwald* [1998], *Lu et al.* [2002], and *Ridley et al.* [1998], through simulations or observations, reported a delay time of 7–8 min for the new IMF orientation to have an effect on the ionosphere after it hits the bow shock. The estimation of the time of the arrival of the IMF transition at the magnetopause involves the orientation of IMF "phase fronts" in the solar wind [*Ridley*, 2000; *Weimer et al.*, 2002, 2003; *Weimer and King*, 2008], the position of bow shock and the magnetopause and some modeling of the propagation in the magnetosheath [*Ruohoniemi et al.*, 2002].

[4] This paper will shows results from a simulated response of the magnetosphere-ionosphere system to a sudden southward turning of IMF orientation using the University of Michigan's MHD code. The detail description of the Block Adaptive-Tree Solar-wind Roe-Type Upwind Scheme (BATS-R-US) is given by *Powell et al.* [1999]. BATS-R-US solves the ideal MHD equations in GSM coordinates, and is coupled to the ionosphere as described by *Ridley et al.* [2004]. The field-aligned currents are computed at 3.5 Earth radii (Re) in the magnetosphere, and mapped down to the ionosphere. The conductivity in the ionosphere is not uniform, rather, it is structured. Namely, the solar generated conductance, nightside conductance and auroral zone con-

[1]Department of Atmospheric, Oceanic and Space Science, University of Michigan, Ann Arbor, Michigan, USA.

0148-0227/09/2008JA013292

ductance, which are dependent on the field-aligned currents, are used (details about the influence of the ionospheric conductance on the magnetosphere are given by *Ridley et al.* [2004]). The flows generated by the ionospheric potential are enforced on a sphere located at 2.5 R_e, where a constant density (28/cc) is also enforced. The magnetic field and temperature are allowed to vary over the 2.5 R_e sphere, but the radial gradient of these quantities is zero. The simulations reported here set both the rotational and magnetic axes of the Earth parallel with the ecliptic north direction. Note that the low density set up at the inner boundary is somewhat different than reality, which is around 1000–10000/cc inside the plasmasphere [*Horwitz et al.*, 1990]. The model is incapable of capturing the sharp change of plasma density at the plasmapause with the resolution used here. Instead, the numerical result shows a slow decrease in the density profile toward the tail. The density in the inner boundary is set up to be much smaller than reality, allowing a relatively correct density outside the plasmapause after the slow decrease, while sacrificing the high-density, corotation-dominated region between the inner boundary (2.5 R_e) and approximately 5 R_e. The input to the model is simply a step function of B_z from 5 nT to −5 nT, while the other solar wind parameters remain constant: solar wind density = 5 cm^{-3}, $V_x = -400$ km/s, $V_y = V_z = B_x = B_y = 0$, and T = 100,000K. Since the IMF and the dipole are symmetric, the simulations are symmetric. Therefore only the northern hemisphere is discussed here.

[5] Determination of the delay time from the encounter of the IMF transition with the bow shock to the dayside reconnection excitation, and subsequently to the ionospheric response will be addressed within this study. Unlike typical situations, a simplified solar wind phase front is modeled, which makes the time estimation work much easier: the propagation in the subsolar region on the upstream Sun-to-Earth line only needs to be considered.

[6] Since the code solves the Poisson equation in the ionosphere, that is, it is treated electrostatically, the ionospheric potential is expected to have a near-simultaneous ionospheric response to the sudden IMF disturbance globally. The ionospheric response, the magnetospheric evolution and ground magnetic perturbations are studied. All the results presented below are in the northern hemisphere owing to the similar phenomena in both hemispheres.

2. Simulation Results

2.1. Ionosphere

[7] Figures 1a–1c show the evolution of the ionospheric potential patterns in northern hemisphere with a 1-min cadence to examine the ionospheric response to the sudden IMF orientation change. The circle plot is centered at the north pole, with the outer boundary at 50° magnetic latitude. The time is labeled at the top left corner and the minimum/maximum potential over the hemisphere is indicated at the bottom left/right corner in each circle plot. The northward-to-southward IMF transition front encounters the bow shock at around 1720 UT at the solar wind speed of 400 km/s. Initially, the ionospheric potential pattern is under northward IMF conditions, with negative (positive) potential cell in the polar cap region in the morning (afternoon) sector and another set in opposite polarity at lower latitudes, although the negative one does not show here.

[8] At 1724 UT, the negative potential cell at lower latitudes starts to ramp up gradually, implying the sharp transition of IMF orientation disturbs the ionospheric system, but to a much smaller extent than what is to come. On the other hand, while the new negative cell is growing in intensity, the one inside the morning polar cap gradually weakens (notice the minimum value of the potential) until around 1730 UT, when the potential cells at lower latitudes dramatically strengthen, indicating that the approaching southward IMF begins to make a major difference. Additionally, the polar cap convection (∼80°) undergoes a reversal of the direction of convection velocity from sunward to antisunward around 1730 UT at local noon and 1732 UT at midnight, which could be considered as a near simultaneous response. This near simultaneous reversal in convection velocities from our simulation is consistent with SuperDARN observations of the line-of-sight velocity when IMF orientation changes suddenly [*Slinker et al.*, 2001; *Ruohoniemi and Greenwald*, 1998]. The two cells at low latitudes continue to increase in magnitude; however, there is almost no evidence for propagation of the convection cells. They center at nearly fixed positions, strengthening in magnitude, which is consistent with the observations by *Ridley et al.* [1998] and *Lu et al.* [2002]. Consequently the well organized two-cell ionospheric potential pattern forms, adjusting to the southward IMF conditions.

[9] Figure 1d (top) shows the cross polar cap potential profile as a function of time. As a parameter reflecting the global response of the ionosphere, the cross polar cap potential (CPCP) is defined as the difference between the maximum and minimum potentials over the hemisphere. Though there are multiple extreme values over the hemisphere, only the maximum positive potential and the minimum negative potential matter in the calculation. The data is obtained from potential patterns with a 10 s cadence. It demonstrates the exact scenario of the evolution of the ionospheric potential: little change before 1724 UT and slight decrease during 1724 UT and 1730 UT indicating that the ionosphere starts to ''feel'' the disturbance at 1724 UT, but to a much smaller extent than after 1729:50 UT (the second vertical dashed line), the time at which the cross polar cap potential dramatically increases, adjusting to a new configuration. Therefore, since the IMF transition front encounters the bow shock, there is a 10-min period after which the southward IMF associated response starts to be observed. As a matter of fact, the time needed varies with the solar wind speed, as will be discussed further in this paper.

[10] By subtracting a potential pattern that is obtained by averaging the potential patterns from 1715 to 1720 UT, a time period during which the ionosphere has not yet been disturbed, the cross polar cap potential profile of the residual potential patterns is shown in Figure 1d (bottom). The vertical dashed lines divide it into three periods after 1724 UT, one in which there is nearly linear change and two in which there exists nearly constant residual cross polar cap potential, similar to patterns reported earlier by *Ridley et al.* [1998] from observations using the assimilative mapping of ionospheric electrodynamics (AMIE) technique [*Richmond and Kamide*, 1988]. The start and stop times of the linear change were determined by adjusting them until the root-mean-square of the difference between the linearly fitted line and the data was minimized. It is found that the linear

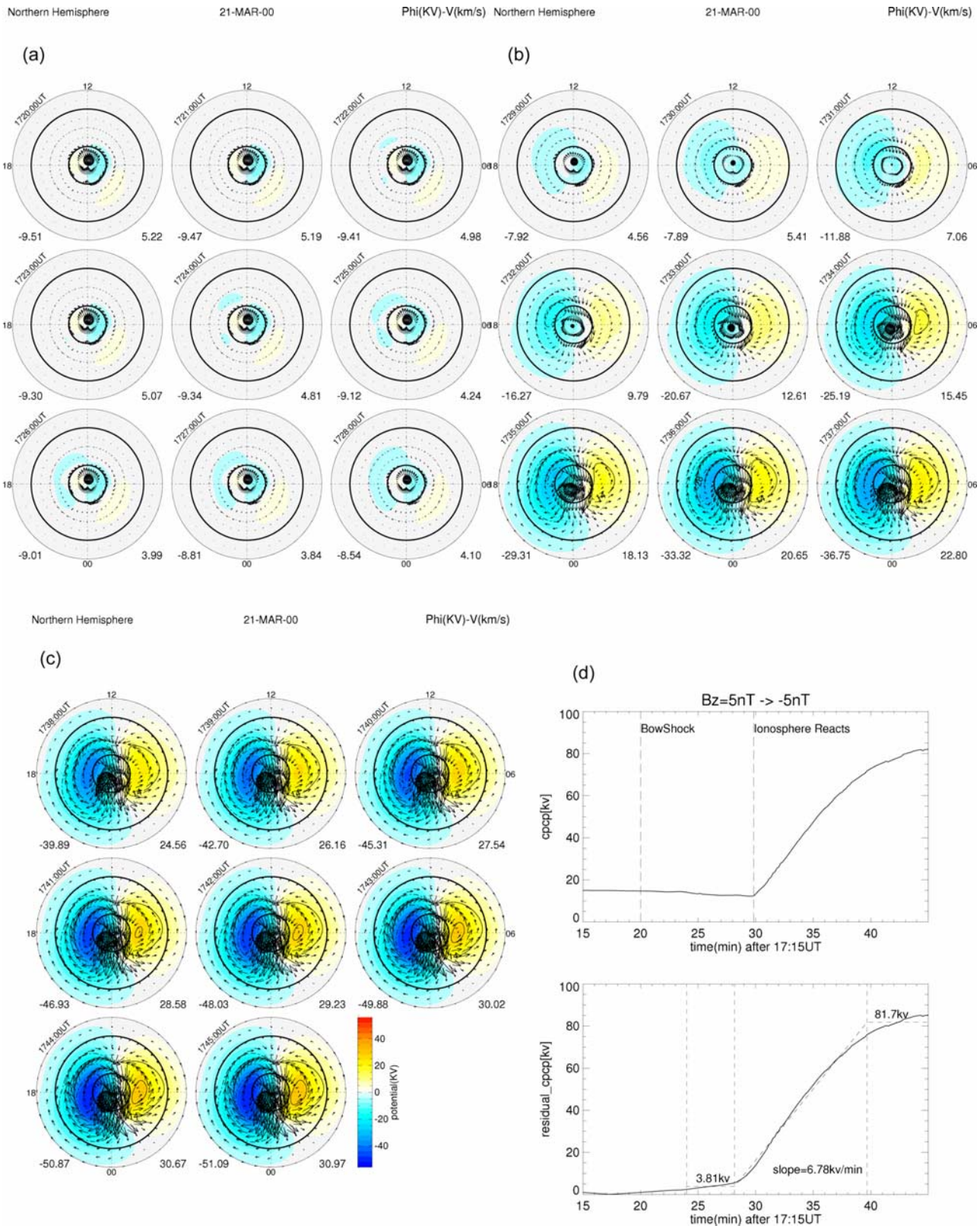

Figure 1. Figures 1a–1c (each consisting of 8 or 9 circle plots) are ionospheric potential patterns, with the color contour representing the potential and the arrows indicating the convection velocities. The time is labeled at the top left corner, and the minimum/maximum potential is indicated at the bottom left/right corner of each circle plot. Figure 1d shows (top) the cross polar cap potential profile and (bottom) residual cross polar cap potential that is obtained by removing an averaged undisturbed pattern.

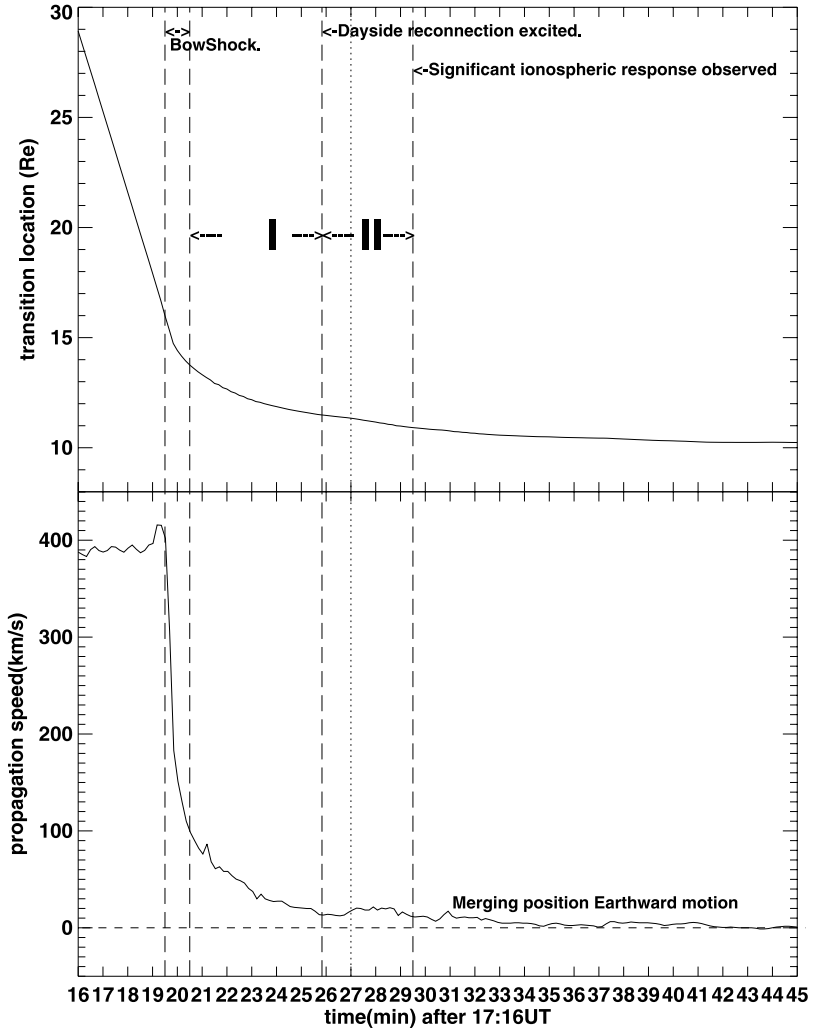

Figure 2. (top) The upstream position of the IMF transition on the Sun-Earth line as a function of time. (bottom) The speed of the transition with respect to the time.

change starts at 1728:10 UT, and ends around 1740 UT with a slope of 6.78 kV/min. The horizontal dashed lines indicate mean values of correspondent periods. The start time of the increase in the residual cross polar cap potential from linearly fitting (at 1728:10 UT) is not consistent with that observed in the original cross polar cap potential profile (at 1729:50 UT). While it is unknown which one should be considered the onset time of the dramatic response in the ionosphere, here we choose to be conservative in terms of this response time; i.e., it is allowed to have an uncertainty of about 2 min. In the text below, we use the later time as the response time in the ionosphere (i.e., 1729:50 UT), although the uncertainty is noted in the final analysis.

2.2. IMF Transition Propagation and Reconnection

[11] In this section, the magnetospheric development is discussed in order to examine the gap between the time in which the IMF discontinuity encounters the bow shock and the time in which the ionosphere starts to experience significant perturbations at 1729:50 UT. The northward to southward IMF transition front travels at the solar wind speed before it encounters the bow shock, and is subsequently slowed down in the magnetosheath. With the newly approaching southward IMF, the northward IMF is simply advected away in the solar wind, while in the magnetosheath, the interaction is more complex. For most northward interplanetary magnetic field lines, the solar wind simply carries them around the magnetosphere, and there is no real interaction with either the southward IMF or the magnetospheric field lines. For other northward field lines, just at the transition between the northward and southward IMF, there exists IMF-to-IMF reconnection. This occurs within the code owing to the sharp gradient in the field sign, increased magnetic field strengths behind the bow shock and a gradient in the flow in the magnetosheath. This interaction between the different IMF regions is mostly likely due to the MHD code's inability to accurately model reconnection. Finally, some northward IMF reaches the magnetopause and undergoes reconnection poleward of the cusp, at which time the field lines become connected to the Earth. These field lines are advected into the reconnection site continuously until the IMF discontinuity reaches the magnetopause, after which time there is no more northward IMF to reconnect, and reconnection above the cusp ceases.

[12] Figure 2 illustrates the upstream position at which the value of B_z changes sign on the Earth-Sun line (i.e., the

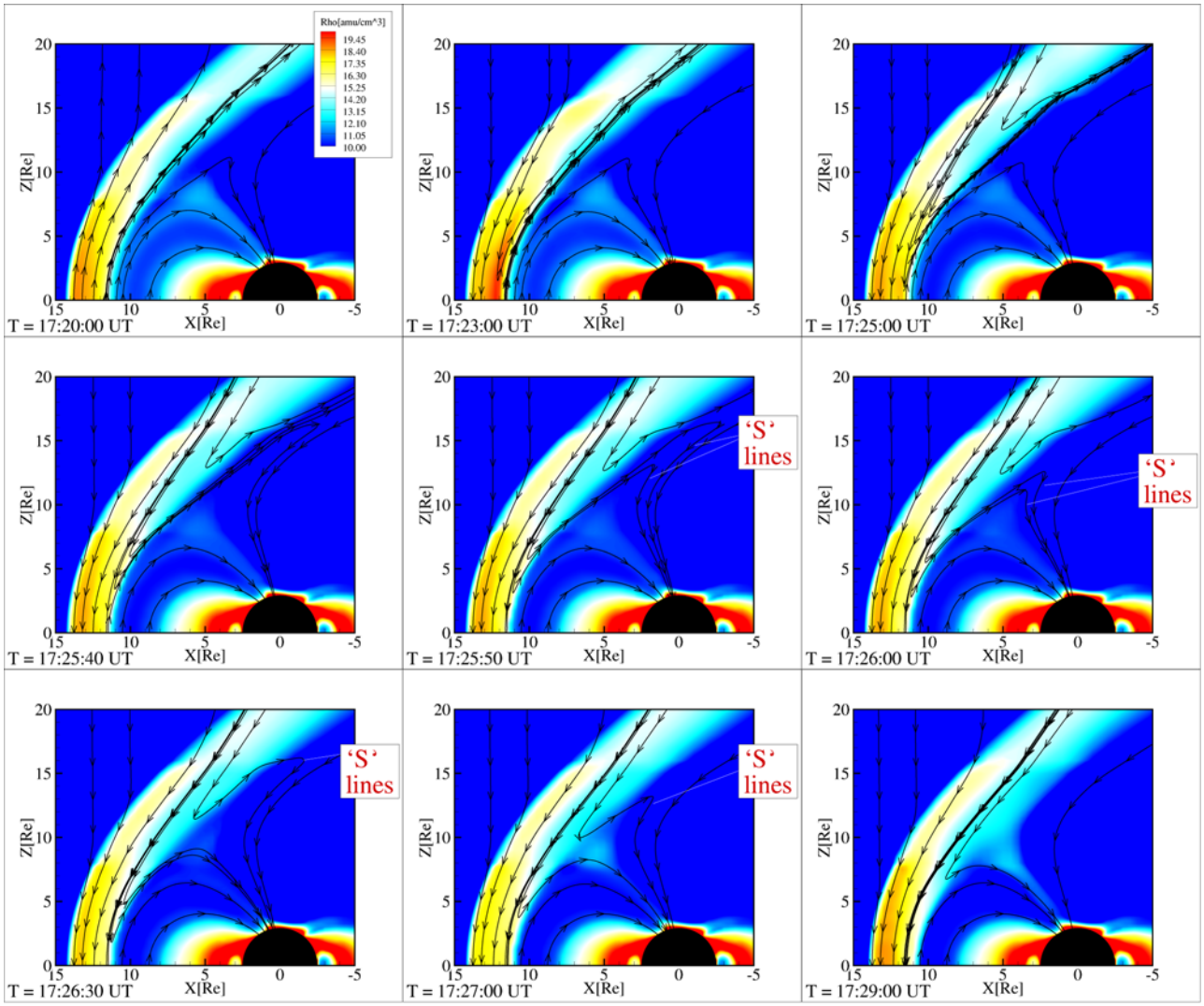

Figure 3. Snapshots of the northern hemispheric magnetosphere in the x-z plane. The color represents the density, while the streamlines are the magnetic field lines (not representing the magnitude of the magnetic field density).

IMF transition front until it reaches the magnetopause, then the actual magnetopause) (top plot) and its propagation speed (bottom plot). The vertical dashed lines indicate the time at which the IMF transition front encounters the bow shock, when it is through the bow shock, when the dayside reconnection is excited, and when the ionosphere starts to respond significantly, respectively. A sharp decrease of the discontinuity speed occurs at 1719:30 UT owing to the bow shock at a distance of 16 R_e away from the Earth, and it takes about 1 min to travel through this boundary, resulting in a downstream speed of ~100 km/s, which is consistent with the Rankine-Hugoniot relations. The propagation of the transition front gradually slows down inside the magnetosheath from 1720:30 until 1725:50 UT when it reaches the subsolar magnetopause (i.e., 5.3 min to propagate through the magnetosheath). The following variation of the speed indicates that the merging position is still approaching the Earth, however generally at a decreasing speed.

[13] The time when the IMF transition front encounters the magnetopause at the subsolar region is picked at the moment the primarily closed dayside geomagnetic field lines start to be opened near the dayside magnetopause. While it is an approximation in finding the first open field line, the time resolution is 10 s, making the uncertainty quite small. Furthermore, the subsolar magnetopause is identified as the place in which B_z changes sign (i.e., dayside subsolar reconnection site), rather than where the plasma flow is zero as done by *Slinker et al.* [2001]. While in this simulation, it is observed that the magnetic discontinuity position is around 0.4 R_e (within 2 grid cells) upstream of the plasma flow velocity transition, this is likely to be caused by numerical diffusion. By zooming into the subsolar region (shown in Figure 3), it is found that the time in which the first field line is merged is sometime between 1725:40 UT and 1725:50 UT. The residing northward IMF is fully advected out of the subsolar region, such that the southward IMF starts to reconnect with geomagnetic field lines, creating newly open field lines. It should be noted that before this time (from 1723 UT on) there is reconnection between IMF field lines within the magnetosheath as described

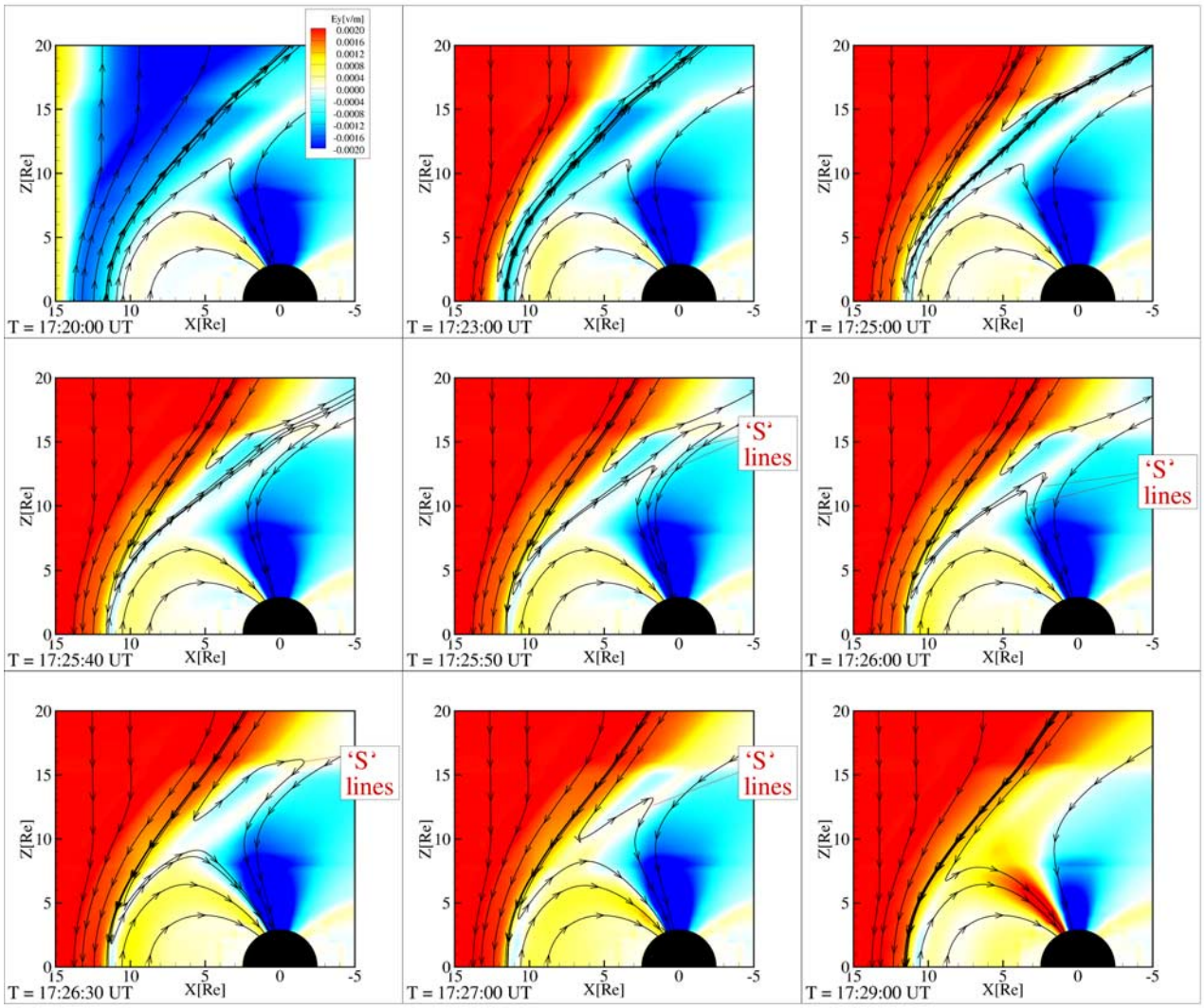

Figure 4. Snapshots of the northern hemispheric magnetosphere in the x-z plane. Red represents the electric field in the Y direction (out of the plane), while blue is the opposite direction. The streamlines are the magnetic field lines (not representing the magnitude of the magnetic field density).

above. This occurs within the simulation owing to the oppositely directed field lines pushing against each other (i.e., there is a velocity gradient through the sheath, so the southward IMF field lines are always moving faster than the northward field lines). Thus, it is 6.3 min between when the southward IMF encountered the bow shock and when the subsolar dayside reconnection occurs.

[14] The deceleration of the transition front inside the magnetosheath (marked as region *I*) can be approximately fitted linearly by simply assuming a constant deceleration velocity a, which is defined as $a = (V_{m.p.} - \frac{1}{4}V_{s.w.})/\Delta T$, where ΔT is the time of propagation from the bow shock inner boundary to the magnetopause, $V_{s.w.}$ is the solar wind speed, and $V_{m.p.}$ is the speed at the magnetopause, which is approximated to be zero. The thickness of the magnetosheath $\Delta X = 2.27R_e$, is obtained from the location profile, therefore, solving the equation $\Delta X = \frac{1}{4}V_{s.w.}\Delta T + \frac{1}{2}a\Delta T^2$ results in a time of propagation of 4.8 min. This is close to that observed in our simulated result (i.e., 5.3 min). However, this linear fitting involves several uncertainties: (1) the magnetopause determined in this study (where B_z changes sign) is actually associated with nonzero plasma flow; (2) the magnetopause is not stationary; instead, it is moving; and (3) the bow shock inner boundary location is defined to be where the plasma flow is slowed down by exactly 3/4, which would be highly approximately without the simulation.

[15] Figure 3 shows snapshots of the development of reconnection in both the dayside and cusp region within the Y = 0 plane. Figure 3 shows only the northern hemisphere, although both hemispheres are modeled. The solid lines are magnetic field lines, which do not represent the magnetic field density, while the color represents the density. After the dayside reconnection is excited near the magnetopause at around 1725:50 UT, it is found that an additional time period of 3–4 min is needed for the system to finish the conversion from the predominant cusp reconnection to the postdominant dayside reconnection at the subsolar region. Geometrically, "S" shaped field lines (as indicated

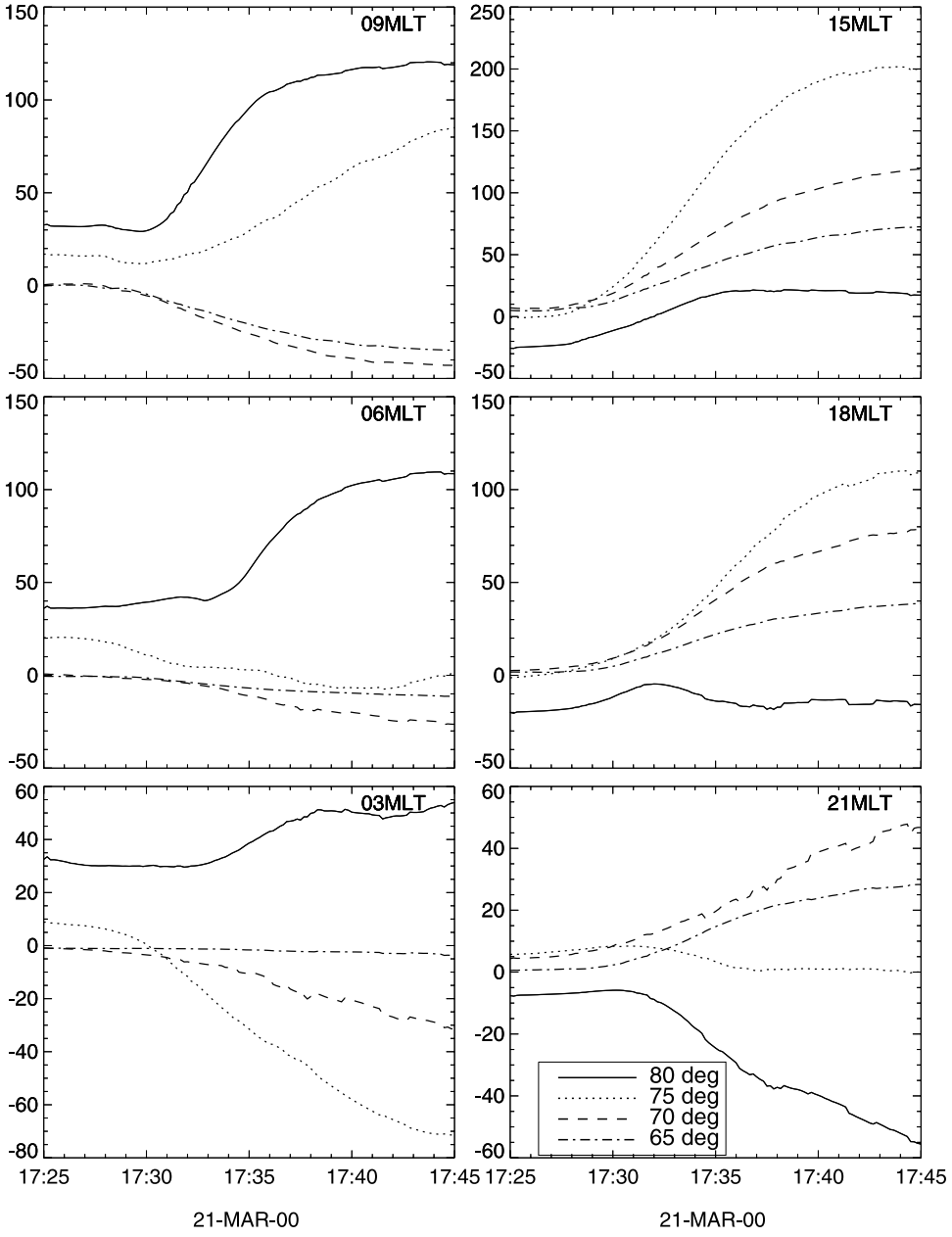

Figure 5. The H component of the ground magnetic perturbations at various local times and latitudes (four lines in each plot). The left plots are in the morning sector, while the right ones are in the afternoon.

in Figure 3) are observed during this period, i.e., a dayside northward geomagnetic line that is stretched to the post-cusp region by the cusp reconnection now also experiences subsolar reconnection caused by the incoming southward IMF line, forming an "S" geometry shape. This geometry dominates the dayside-to-cusp meridian region from 1725:50 UT to 1729 UT until field lines in "S" shape are unwound by the plasma flow ejected from the subsolar reconnection.

[16] During the northward IMF period, the plasma just equatorward and sunward of the cusp have a high density, which can be observed by the color inside the magnetosphere in Figure 3. Before and at 1725:40 UT, the main density transferred to the magnetosphere from the solar wind is from the cusp reconnection as observed in Figure 3: the relatively high density branch (light blue) in the cusp region inside the magnetosphere. After 1725:40 UT, the "path" for density injection is eliminated, implying that the cusp reconnection is weakened and destroyed by the lack of northward IMF and the outflow from the subsolar reconnection. Around 1727 UT, the injection "path" with higher density appears again, however, it is now interlinked with the magnetopause. This new "path" for high-density plasma is generated by the subsolar reconnection. This kind of evolution of the high-density "path" occurs simultaneously with the conversion between the two types of reconnection.

[17] As the electric field in the magnetosphere plays an important role in determining the ionospheric convection, the electric field in GSM Y (i.e., E_y) direction is shown in Figure 4, which has the same format as Figure 3. Initially,

the electric field is dusk-to-dawn (blue) in the solar wind as well as above the polar cap as well known in northward IMF conditions. After the southward IMF encounters the magnetosphere, notice that the dusk-to-dawn (blue) electric field along the magnetopause gradually fades away, which implies the northward IMF is being replaced by the approaching southward IMF. After the subsolar reconnection is excited around 1725:40 UT, the direction of the electric field changes to dawn-to-dusk (yellow) at the place where the subsolar reconnection associated high-density flow is observed from Figure 3 after 1727 UT, and this electric field starts to dominate the cusp region, weakening the dusk-to-dawn (blue) electric field in the postcusp region which implies the reverse convection in the ionosphere is being supplanted by antisunward convection.

[18] Since the primary large-scale response of the ionosphere that is associated with the southward IMF condition emerges at 1729:50 UT, as mentioned in section 1, and the dayside reconnection starts at 1725:50 UT near the subsolar magnetopause, it indicates that it takes about 4 min for the disturbance caused by the subsolar reconnection to propagate down to the ionosphere. This period is marked as region *II* in the Figure 2. It is associated with two successive processes (they are separated by the vertical dotted line in Figure 2): (1) the cusp reconnection is destroyed from 1725:40 UT to 1727 UT, as indicated by the high-density flow "path" caused by cusp reconnection weakening and then disappearing as well as the fading of the dusk-to-dawn electric field associated with the cusp reconnection along the magnetopause; and (2) the new high-density flow generated by the dayside reconnection forms and spreads down into the magnetosphere after 1727 UT and the electric field is changed to dawn-to-dusk. The ionosphere then experiences a significant disturbance after 1729:50 UT. Therefore, combining with the previous 6.3-min travel time between the bow shock encounter and when the dayside reconnection initiates (1 min of traveling through the bow shock and 5.3 min through the magnetosheath), the total time delay between the discontinuity encountering the bow shock and when the ionosphere starts to respond is 10.3 min.

2.3. Ground Magnetic Perturbations

[19] The ionospheric response is also detected in the ground magnetic perturbations, shown in Figure 5. Different plots are at various magnetic local times, while different traces represent the H component of ground magnetic perturbations at various magnetic latitudes. The ground magnetic field perturbations are derived from Hall currents over the entire hemispheric ionosphere by Biot-Savart integral. Most locations show monotonic increases in the magnitude to a roughly constant value. Initial responses appear around 1729 UT nearly globally from dayside to nightside, from high latitude to low latitude. However, the rate of change that is associated with the reconfiguration differs at different latitudes: generally speaking, the maximum magnetic perturbations arrive at the higher latitudes first and then at lower latitudes. Furthermore, the simulation shows a delayed propagation of the maximum magnetic perturbations from local noon to the nightside after the initial responses. These results are in consistence with the observations reported by *Lu et al.* [2002] (and references therein), who thoroughly studied and interpreted the two-stage ionospheric response (i.e., fast initial onset and the slow final reconfiguration) to the IMF southward turning, as well as the dayside-to-nightside propagation of the maximum magnetic perturbations through cross-correlation analysis.

3. Discussion and Summary

[20] While the main point of this study is not focused on the nearly simultaneously global response of the ionospheric potential to changes in the IMF, this is observed. Using the model, one would expect some type of globally simultaneous response, since the ionospheric electric field is assumed to be a potential field, which implies an instantaneous communication time across the ionosphere. Still, the results from the model match observational results, in the potential [e.g., *Ridley et al.*, 1998] convection [e.g., *Shepherd et al.*, 1999; *Murr and Hughes*, 2001; *Ruohoniemi and Greenwald*, 1998], and ground-based magnetic perturbations [*Lu et al.*, 2002], indicating that the model is simulating the global response in a physically consistent manner.

[21] The main goal of this study is to examine the time delays related to the IMF discontinuity interacting with the bow shock and magnetopause, and finally influencing the ionospheric convection. Note that the delay time studied in this paper is the time period between when the north-to-south transition of IMF encounters the bow shock and when the ionosphere responds to the IMF disturbance. This delay time is different from those discussed in previous studies that mainly focused on the time difference between the dayside and nightside responses in the ionosphere.

[22] There are two issues that are related with the way we determine the time delay that require clarification: (1) the time at which the IMF change reaches at the magnetopause and (2) the time that the ionosphere demonstrates a response to the IMF disturbance. The arrival of the IMF change at the magnetopause is determined by the time in which the first open field line is generated by the dayside subsolar reconnection. *Slinker et al.* [2001] defined the magnetopause as being the transition point between oppositely directed flows, and determined the time of arrival as when the front reached this boundary. While, with infinite resolution, these locations should be exactly the same, they are not in our simulation, differing by 1–2 grid cells (or 0.4 Re), with the velocity boundary more Earthward than the reconnection boundary. This is purely numerical. The time of the first reconnection was utilized in the analysis, because it is a more physically meaningful event than the crossing of a numerical boundary.

[23] The time in which the ionosphere starts to respond to the IMF change is also debatable. The ionosphere responds at a time determined either by taking the point in which the cross polar cap potential suddenly increases or by a linearly fitting approach to the residual cross polar cap potential; however, there is a discrepancy: the fitting approach obtains a response time about 1.7 min earlier than that observed in cross polar cap potential profile, and it is uncertain which start time is the correct one to use.

[24] With the approaches discussed above, it is found that, besides the approximate 6 min propagation time from the IMF discontinuity's encounter with the bow shock to the subsolar magnetopause, another 2.3–4.0 min are required for the newly southward IMF to finally influence the ionosphere. This time delay is due to the time it takes for the predominant

Table 1. Propagation Time of the IMF Transition Front Through the Subsolar Region With Different Solar Wind Speeds[a]

SW Speed (km/s)	$\Delta T0$	$\Delta T1$	$\Delta T2$	Total	$R_{M.sheath}$	$\Delta T1_{lin}$
300	1.7	8.7	4.3(−1.1)	14.6(−1.1)	2.87	8.1
400	1.0	5.3	4.0(−1.7)	10.3(−1.7)	2.27	4.8
500	0.8	4.0	3.2(−1.3)	8.0(−1.3)	2.0	3.4
600	0.7	3.0	2.5(−1.1)	6.2(−1.1)	1.87	2.7

[a]Different time periods represent the following: $\Delta T0$, bow shock boundary; $\Delta T1$, magnetosheath; $\Delta T2$, the time the ionosphere starts to significantly respond after the dayside reconnection is excited by southward IMF; $R_{M.sheath}$, the thickness of the magnetosheath; $\Delta T1_{lin}$, time in the magnetosheath by linearly fitting. The unit of these time periods is minutes, and the unit of the thickness of the magnetosheath is R_e.

cusp reconnection to stop and be replaced by the dayside subsolar reconnection, as well as the time it takes for the dayside perturbations to propagate down to the ionosphere via an Alfvén wave.

[25] It is found that within the simulation, the IMF takes about 1 min to slow down through the bow shock. The transition then propagates through the magnetosheath, slowing all of the time. Once it encounters the magnetopause, reconnection is initiated, and the discontinuity (now the magnetopause) continues to move earthward for over 10 min. This motion does not stop until tail reconnection occurs, which produces convection of closed field lines back to the dayside magnetosphere, counterbalancing the erosion of the geomagnetic field lines on the dayside. However, this additional time for the magnetopause to move inward does not seem to affect the time delay between when reconnection begins and when the ionosphere starts to respond, but it may affect how long it takes the ionosphere to completely change. These times appear to be related, since the Earthward motion stops around 1742 UT (Figure 2), while the ionosphere is mostly changed by 1740–1744 UT. While this is purely speculative at this point, it is an area that could be examined more closely in the future with many more simulations or statistical analysis of data.

[26] As the propagation time from the bow shock to the magnetopause depends on the solar wind speed, a few more simulations with different solar wind speeds are conducted. The times in which the IMF transition encounters the magnetopause and the ionosphere responds are determined in the same way as described above. The results are listed in Table 1. $\Delta T0$ is the time it takes for the IMF transition front to travel through the bow shock boundary, and $\Delta T1$ is the propagation time inside the magnetosheath, where the starting time is picked right after the solar wind speed is reduced by 3/4. $\Delta T2$ is the time difference between when the ionosphere starts to significantly respond and when the dayside reconnection is excited at the magnetopause, where the response time is determined from the cross polar cap potential profile, instead of from the linearly fitting of residual cross polar cap potential profile, with the number in the parenthesis representing the difference between the two methods. The total time includes the time from the discontinuity encountering the bow shock to the reaction in the ionosphere, i.e., the sum of the first three times. The period of propagation ($\Delta T1_{lin}$) within the magnetosheath is also fitted linearly assuming a constant deceleration, with the magnetosheath thickness ($R_{M.sheath}$) varying with the solar wind speed. The times that are needed to travel through the bow shock boundary, then within the magnetosheath, and eventually to influence the ionosphere respectively, are all shorter for higher solar wind speeds. These times are consistent with other studies that have observational estimated the magnetopause-ionosphere communication time. For example, *Watanabe et al.* [2000] reported a 2–3 min communication time after the IMF change at the subsolar magnetopause with a solar wind speed around 600 km/s.

[27] This study shows that some of the time delay between when reconnection is initiated and when the ionosphere responds (i.e., $\Delta T2$) is due to the time it takes to replace the preexisting cusp reconnection by the dayside subsolar reconnection, and the time needed to propagate the dayside disturbance down to the ionosphere via an Alfvén wave.

[28] It should be noted that this work idealizes the problem in many aspects, including ideal IMF components, constant solar wind parameters and no dipole tilt. The IMF B_y has significant influence on the development of the ionosphere [*Saunders et al.*, 1992]. The time delay of the ionospheric response to the sudden IMF change may be different and more complex when there is an IMF B_y, since the direction of the cusp is not aligned with the noon-midnight meridian as the case in this work. The cusp orientation highly depends on the angle between B_z and B_y [*Nemeèek and Šafránková*, 2008; *Crooker*, 1979], so the delay time may be longer than that in this paper. Furthermore, an angle between the rotation axis and the magnetic dipole axis or a tilted IMF causes different IMF lines to be involved in the two cusp reconnection processes, resulting in two open field lines, rather than one single closed line as in this study. In such a situation, the initialization of the dayside reconnection does not occur at the subsolar point any more; instead, it may be more difficult to determine the position and the time in which the IMF discontinuity reaches at the magnetopause. Another note about the time estimation is that owing to numerical diffusion, the bow shock is actually thicker than that in nature for an exactly perpendicular shock. Therefore, the delay time may be slightly overestimated in our study.

[29] **Acknowledgments.** This work is supported by NSF grant 0639336.

[30] Zuyin Pu thanks Ling-Hsiao Lyu and another reviewer for their assistance in evaluating this paper.

References

Cowley, S. W. H., and M. Lockwood (1992), Excitation and decay of solar wind-driven flows in the magnetosphere-ionosphere system, *Ann. Geophys.*, *10*, 103–115.

Crooker, N. U. (1979), Dayside merging and cusp geometry, *J. Geophys. Res.*, *84*, 951–959.

Horwitz, J. L., R. H. Comfort, and C. R. Chappell (1990), A statistical characterization of plasmasphere density structure and boundary locations, *J. Geophys. Res.*, *95*, 7937–7947.

Khan, H., and S. W. H. Cowley (1999), Observations of the repsonse time of high-latitude convection to variations in the interplanetary magnetic field using EISCAT and IMP-8 data, *Ann. Geophys.*, *17*, 1306–1335.

Lockwood, M., A. P. van Eyken, B. J. I. Bromage, D. M. Willis, and S. W. H. Cowley (1986), Eastward propagation of a plasma convection enhancement following a southward turning of the interplanetary magnetic field, *Geophys. Res. Lett.*, *13*, 72–75.

Lopez, R. E., M. Wiltberger, J. G. Lyon, C. C. Goodrich, and K. Papadopoulos (1999), MHD simulations of the response of high-latitude potential patterns and polar cap boundaries to sudden southward turnings of the interplanetary magnetic field, *Geophys. Res. Lett.*, *26*, 967–970.

Lu, G., T. E. Holzer, D. Lummerzheim, J. M. Ruohoniemi, P. Stauning, O. Troshichev, P. T. Newell, M. Brittnacher, and G. Parks (2002), Ionospheric response to the interplanetary magnetic field southward turning: Fast onset and slow reconfiguration, *J. Geophys. Res.*, *107*(A8), 1153, doi:10.1029/2001JA000324.

Murr, D. L., and W. J. Hughes (2001), Reconfiguration timescales of ionospheric convection, *Geophys. Res. Lett.*, *28*, 2145–2148.

Nishitani, N., T. Ogawa, N. Sato, H. Yamagishi, M. Pinnock, J.-P. Villain, G. Sofko, and O. Troshichev (2002), A study of the dusk convection cell's response to an IMF southward turning, *J. Geophys. Res.*, *107*(A3), 1036, doi:10.1029/2001JA900095.

Němeček, Z., and J. Šafránková (2008), IMF control of the high-altitude cusp dynamics, *Adv. Space Res.*, *41*, 92–102.

Powell, K. G., P. L. Roe, T. J. Linde, T. I. Gombosi, and D. L. D. Zeeuw (1999), A solution-adaptive upwind scheme for ideal magnetohydrodynamics, *J. Comput. Phys.*, *154*, 284–309.

Richmond, A. D., and Y. Kamide (1988), Mapping electrodynamic features of the high-latitude ionosphere from localized observations: Technique, *J. Geophys. Res.*, *93*, 5741–5759.

Ridley, A. J. (2000), Estimation of the uncertainty in timing the relationship between magnetospheric and solar wind processes, *J. Atmos. Sol. Terr. Phys.*, *62*, 757–771.

Ridley, A. J., C. R. Clauer, G. Lu, and V. O. Papitashvili (1998), A statistical study of the ionospheric convection response to changing interplanetary magnetic field conditions using the assimilative mapping of ionospheric electrodynamics technique, *J. Geophys. Res.*, *103*, 4023–4039.

Ridley, A. J., T. I. Gombosi, and D. L. D. Zeeuw (2004), Ionospheric control of the magnetospheric configuration: Conductance, *Ann. Geophys.*, *22*, 567–584.

Ruohoniemi, J. M., and R. A. Greenwald (1998), The response of high-latitude convection to a sudden southward IMF turning, *Geophys. Res. Lett.*, *25*, 2913–2916.

Ruohoniemi, J. M., S. G. Shepherd, and R. A. Greenwald (2002), The response of the high-latitude ionosphere to IMF variations, *J. Atmos. Terr. Phys.*, *64*, 159–171.

Saunders, M. A., M. P. Freeman, D. J. Southwood, S. W. H. Cowley, M. Lockwood, J. C. Samson, C. J. Farrugia, and T. J. Hughes (1992), Dayside ionospheric convection changes in response to long-period interplanetary magnetic field oscillations: Determination of the ionospheric phase velocity, *J. Geophys. Res.*, *97*, 19,373–19,380.

Shepherd, S. G., R. A. Greenwald, and J. M. Ruohoniemi (1999), A possible explanation for rapid, large-scale ionospheric responses to southward turnings of the IMF, *Geophys. Res. Lett.*, *26*, 3197–3200.

Slinker, S. P., J. A. Fedder, J. M. Ruohoniemi, and J. G. Lyon (2001), Global MHD simulation of the magnetosphere for November 24, 1996, *J. Geophys. Res.*, *106*, 361–380.

Todd, H., S. W. H. Cowley, M. Lockwood, D. M. Willis, and H. Lühr (1988), Response time of the high-latitude dayside ionospheric convection to sudden changes in the north-south component of the IMF, *Planet. Space Sci.*, *36*, 1415–1428.

Watanabe, M., N. Sato, R. A. Greenwald, M. Pinnock, M. R. Hairston, R. L. Rairden, and D. J. McEwen (2000), The ionospheric response to interplanetary magnetic field variations: Evidence for rapid global change and the role of preconditioning in the magnetosphere, *J. Geophys. Res.*, *105*, 22,955–22,978.

Weimer, D. R., and J. H. King (2008), Improved calculations of interplanetary magnetic field phase front angles and propagation time delays, *J. Geophys. Res.*, *113*, A01105, doi:10.1029/2007JA012452.

Weimer, D. R., D. M. Ober, N. C. Maynard, W. J. Burke, M. R. Collier, D. J. McComas, N. F. Ness, and C. W. Smith (2002), Variable time delays in the propagation of the interplanetary magnetic field, *J. Geophys. Res.*, *107*(A8), 1210, doi:10.1029/2001JA009102.

Weimer, D. R., D. M. Ober, N. C. Maynard, M. R. Collier, D. J. McComas, N. F. Ness, C. W. Smith, and J. Watermann (2003), Predicting interplanetary magnetic field (IMF) propagation delay times using the minimum variance technique, *J. Geophys. Res.*, *108*(A1), 1026, doi:10.1029/2002JA009405.

A. J. Ridley and Y. Yu, Department of Atmospheric, Oceanic and Space Science, University of Michigan, 1417 Space Research Building, Ann Arbor, MI 48109, USA. (yiqunyu@umich.edu)